N°45

Reprinted from

ENGINEERING GEOLOGY

AN INTERNATIONAL JOURNAL

Engineering Geology 49 (1998) 1–13

A combined hillslope hydrology/stability model for low-gradient clay slopes in the Italian Dolomites

M.G. Angeli [a], J. Buma [b,*], P. Gasparetto [c], A. Pasuto [d]

[a] *IRPI–CNR, Via Madonna Alta 26, 06128 Perugia, Italy*
[b] *Department of Physical Geography, University of Utrecht, PO Box 80115, 3508 TC Utrecht, The Netherlands*
[c] *IRPI–CNR, Corso Stati Uniti 4, 35127 Padova, Italy*
[d] *IRPI–CNR, Corso Stati Uniti 4, 35127 Padova, Italy*

Received 26 August 1996; accepted 15 May 1997

ELSEVIER

ENGINEERING GEOLOGY

Aims and scope of the journal

The Journal is an international medium for the publication of original studies, case histories, and comprehensive reviews in the field of Engineering Geology. Included are all geological studies that can be relevant to engineering, environmental concerns and safety. The editors will consider papers on subjects such as aerial photograph interpretation for land usage, control of hazards from geological processes (earthquakes, floods, river diversions, land slips, etc.), assessment of geological factors affecting river behavior, rehabilitation of groundwater supplies, field assessment of earthquake-generating faults, criteria for ground storage of hazardous wastes, techniques of reconnaissance, geological mapping for engineering, etc. To maintain a high scientific level all papers will be refereed by the Editorial Board. An "Opinion section" is provided for timely expression of views and ideas. These submissions will be reviewed for reasonableness by an Editor-in-Chief and published as rapidly as possible. The objective is to produce a journal with international coverage that will contribute to the development of engineering geology as a profession.

Publication information

Engineering Geology (ISSN 0013-7952). For 1998 volumes 47–49 are scheduled for publication. Subscription prices are available upon request from the publisher. Subscriptions are accepted on a prepaid basis only and are entered on a calendar year basis. Issues are sent by surface mail except to the following countries where air delivery via SAL is ensured: Argentina, Australia, Brazil, Canada, Hong Kong, India, Israel, Japan, Malaysia, Mexico, New Zealand, Pakistan, PR China, Singapore, South Africa, South Korea, Taiwan, Thailand, USA. For all other countries airmail rates are available upon request. Claims for missing issues must be made within six months of our publication (mailing) date. Please address all your requests regarding orders and subscription queries to: Elsevier Science B.V., Customer Support Department, P.O. Box 211, 1000 AE Amsterdam, The Netherlands. Fax: +31 20 485 3432.

Advertising information

Advertising orders and enquiries may be sent to: Elsevier Science B.V., Advertising Department, The Boulevard, Langford Lane, Kidlington, Oxford, OX5 1GB, UK, tel.: +44 (0) 1865 843565, fax: +44 (0) 1865 843976. *In the USA and Canada*: Weston Media Associates, attn. Daniel Lipner, P.O. Box 1110, Greens Farm, CT 06436-1110, USA, tel.: +1 (203) 261 2500, fax: +1 (203) 261 0101. *In Japan*: Elsevier Science Japan, Marketing Services, 1-9-15 Higashi-Azabu, Minato-ku, Tokyo 106, Japan, tel.: +81 3 5561 5033; fax: +81 3 5561 5047.

0013-7952/98/$19.00

ELSEVIER

A combine

[b] *Department of*

Abstract

The temporal tren
function of precipitat
and surficial displace
occurrence of preferei
a less permeable, con
linear reservoir mode
lower outlet drains th
in time. This was don
which controls the thi
output from the mod
taking into account a
validation on 3 years
estimates of cumulati
underlying the model
typical of many other

Keywords: Displacem

1. Introduction

In order to assess
ous areas related to
ceptual understan
precipitation, pore

* Corresponding author.

0013-7952/98/$19.00 © 1
PII S0013-7952(97)0

ELSEVIER

Engineering Geology 49 (1998) 1–13

ENGINEERING GEOLOGY

A combined hillslope hydrology/stability model for low-gradient clay slopes in the Italian Dolomites

M.G. Angeli [a], J. Buma [b,*], P. Gasparetto [c], A. Pasuto [d]

[a] *IRPI–CNR, Via Madonna Alta 26, 06128 Perugia, Italy*
[b] *Department of Physical Geography, University of Utrecht, PO Box 80115, 3508 TC Utrecht, The Netherlands*
[c] *IRPI–CNR, Corso Stati Uniti 4, 35127 Padova, Italy*
[d] *IRPI–CNR, Corso Stati Uniti 4, 35127 Padova, Italy*

Received 26 August 1996; accepted 15 May 1997

Abstract

The temporal trend of displacement of a landslide on a low-gradient clay slope in the Italian Dolomites as a function of precipitation was simulated with a combined hydrological–slope stability model based on groundwater and surficial displacement observations. Piezometric records and lithological profiles from boreholes suggest the occurrence of preferential groundwater flow through a very permeable top layer of about 1 m thickness, which overlies a less permeable, compact clay layer penetrated by dead-end cracks. To simulate groundwater levels in this system, a linear reservoir model with two outlets was applied, where the upper outlet drains the permeable top layer, and the lower outlet drains the dead-end cracks in the clay layer. The reservoir was assigned a bottom boundary level varying in time. This was done to represent an inferred yearly fluctuation of a matric groundwater level due to regional flow, which controls the thickness of the unsaturated part of the clay layer absorbing water from the cracks. Groundwater output from the model was used in a visco-plastic stability model to simulate the velocity of landslide movement, taking into account a phenomenon of strength regain that occurs in the clays along the slip surfaces. Calibration and validation on 3 years of groundwater and displacement data showed that both models yield good results. Thus, good estimates of cumulative landslide displacement were obtained as a function of precipitation. The general concepts underlying the models offer possibilities for regionalization because from a geological point of view, this landslide is typical of many others in the Dolomites. © 1998 Elsevier Science B.V.

Keywords: Displacements; Dolomites; Groundwater; Landslides; Models; Monitoring

1. Introduction

In order to assess landslide hazard in mountainous areas related to meteorological factors, a conceptual understanding of relations between precipitation, pore pressures and stability of hillslopes is required. However, landslides are difficult phenomena to investigate because they are commonly geologically and morphologically very complex. Consequently, many models for simulating the temporal behaviour of landslides remain confined to a specific site for which all particular features are considered.

This paper presents an attempt to model the

* Corresponding author.

PII S0013-7952(97)00033-1

temporal activity of a slow-moving landslide on a low-gradient clay slope in the Dolomites (north-east Italy). The models applied were kept as simple as possible to enable future regionalization; many landslides occur on geologically and morphologically similar slopes in this area (Angeli et al., 1992, 1996c). On the basis of permanent monitoring of precipitation, groundwater levels and surficial displacement, a concept for the temporal behaviour of the landslide in relationship to meteorology is proposed. This is incorporated into a combined numerical hillslope hydrology–stability model. A linear reservoir model for simulation of groundwater levels was coupled to a visco-plastic stability model. Because the latter model is discussed in detail by Angeli et al. (1996b), the focus will be on the hydrological model, and the combination of the two models.

2. Alverà landslide study area

The Alverà landslide is situated near Cortina d'Ampezzo in the Dolomites. Fig. 1 shows its location and Fig. 2 shows a schematic geological cross-section. The landslide is described in detail by Angeli et al. (1992), Deganutti and Gasparetto (1992), Gasparetto et al. (1994), Gasparetto et al. (1995), and Angeli et al. (1996a,c). The geological structure of the area is characterized by a repeated succession of dolomitic and pelitic rocks. This structure has strongly influenced the morphological evolution of the area since the retreat of the Würmian glaciers (Panizza et al., 1996): the landscape is dominated by steep dolomitic walls (Dolomia Principale) with gentler slopes at their base, developed in less-resistant formations. The landslide developed on a low-gradient slope (average inclination 7.3°) and involves lithotypes belonging to the San Cassiano Formation, which consists mainly of interbedded marls, shales and grey-coloured calcarenites. In the study area, a particularly clayey facies of this formation prevails. As a result of its nature, the San Cassiano Formation is subject to intense weathering, with the consequent production of a clayey–silty material which is largely involved in several landslides, including the Alverà landslide. The vegetation on the landslide consists of tall grass and patches of reed. Laboratory tests, carried out on samples

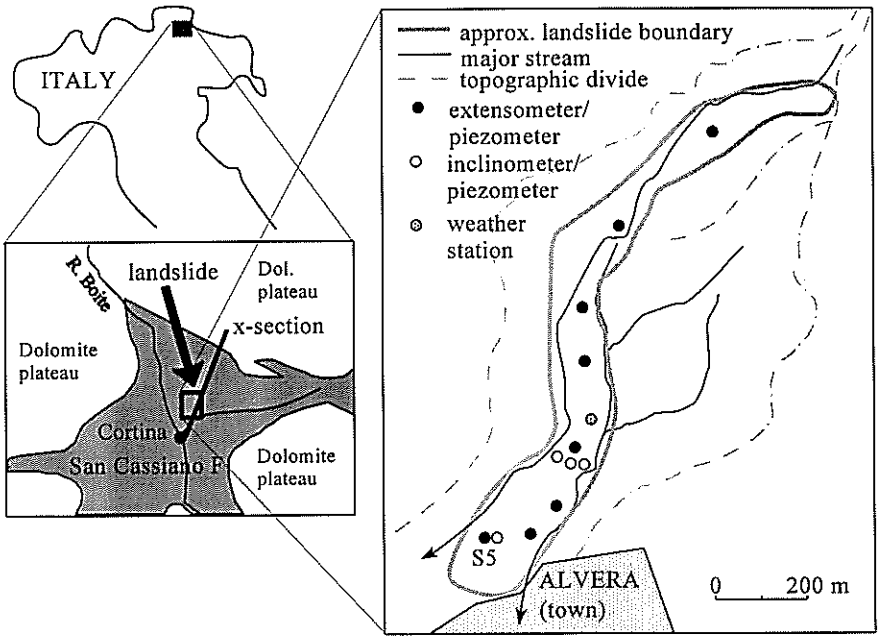

Fig. 1. Geographical setting of the Alverà landslide.

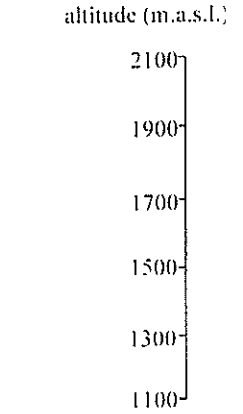

Fig. 2. Schematic geologi
Carnian–Raethian p.p.) v
Carnian) pelites and marls
crystalline dolomites; (4)
and grey-coloured calcare

from various depths
surface, provided the

Since 1989, a n
installed consisting
equipped with electr
inclinometers and 1
the continuous meas
ment (see Fig. 1). T
30 m in depth. The
piezometer tube are
rated. Moreover, a
topographic survey
movements to be de
tion was also set up i
(both rainfall and
temperature and sn
recorded automatica

Table 1
Geotechnical characterist

Bulk unit weight	
Clay content	
Liquid limit	
Plasticity index	
Residual shear angle	

is described in detail
nutti and Gasparetto
)4), Gasparetto et al.
'6a,c). The geological
:terized by a repeated
l pelitic rocks. This
ıced the morphologi-
ce the retreat of the
: al., 1996): the land-
:ep dolomitic walls
entler slopes at their
:ant formations. The
low-gradient slope
d involves lithotypes
ıo Formation, which
ed marls, shales and
n the study area, a
ıis formation prevails.
, the San Cassiano
nse weathering, with
f a clayey–silty mate-
in several landslides,
e. The vegetation on
grass and patches of
'ied out on samples

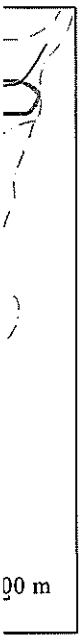

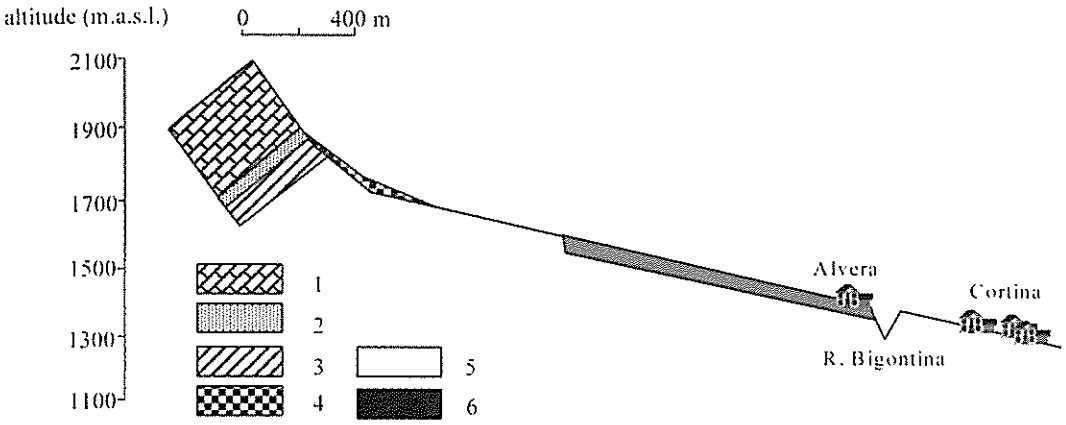

Fig. 2. Schematic geological cross section of the slope affected by the Alverà landslide. Legend: (1) Dolomia Principale (Upper Carnian–Raethian p.p.) white and grey cyclic dolomites with stromatholitic and massive lithozones; (2) Raibl Formation (Upper Carnian) pelites and marls, limestones and microcrystalline dolomites; (3) Dolomia Cassiana (Lower Carnian) white greyish, massive crystalline dolomites; (4) Quaternary deposits (scree slope); (5) San Cassiano Formation (Lower Carnian) interbedded marls, shales and grey-coloured calcarenites; and (6) landslide body.

from various depths in the slope and from the slip surface, provided the geotechnical data in Table 1.

Since 1989, a monitoring system has been installed consisting of 11 open-pipe piezometers equipped with electric pressure transducers, four inclinometers and 11 steel wire extensometers for the continuous measurement of landslide displacement (see Fig. 1). The boreholes range from 9 to 30 m in depth. The top 2 m of each open-pipe piezometer tube are closed, the remainder is perforated. Moreover, a network of benchmarks for topographic surveying has allowed superficial movements to be detected. A meteorological station was also set up in order to record precipitation (both rainfall and snow water equivalent), air temperature and snow cover thickness. Data are recorded automatically every 10 min.

Surficial movement averages about 0.08 m year^{-1}. The inclinometric measurements revealed that a narrow zone at 5 m depth below the ground surface accounts for 75% of the recorded deformation, while the remaining 25% is caused by a broad creep zone between 17 and 25 m depth.

3. A concept for the temporal behaviour of the landslide

First, some observations relating to the hydrology of the landslide are summarized, based on the monitoring data and some additional field measurements. Four piezometers show no significant response to any meteorological event. Of these,

Table 1
Geotechnical characteristics of the Alverà landslide (Angeli et al., 1996b)

Bulk unit weight	Any depth	18.7 kN m^{-3}
Clay content	Any depth	30–63%
	Shear surface	68–71%
Liquid limit	Any depth	47.7–71.0%
	Shear surface	91.5–99.1%
Plasticity index	Any depth	15.5–33.0%
	Shear surface	44.5–51.1%
Residual shear angle	Any depth	16.7° (direct shear test)
	Shear surface	15.9° (ring shear test)

two are known to be broken by ground movement and the perforated section of another was blocked by excessive benthonite sealing. All four were excluded from further analysis. A representative example of the remaining piezometer records, the record of S5, is shown in Fig. 3, together with the corresponding extensometric record. The following features in the records are striking:

(1) Above a certain "threshold" level, groundwater fluctuations are invariably rapid (within a few days), strong (up to almost 1 m) and of short duration (within days), following liquid precipitation (Hennrich, 1995). The threshold level lies between −0.40 and −1.50 m in the piezometers; in S5 it is about −1.00 m. Peaks following snowmelt in early spring have a longer duration.

(2) The fall of groundwater below this level strongly depends on the season. In winter, no fall at all is observed even when (liquid) precipitation is zero for weeks. In summer, the fall of groundwater is much faster, even after very large precipitation events. In the case of a sufficiently large event, a groundwater rise can be as strong and as rapid as in other seasons, no matter how low the initial level is. Other summer events seem not to be large enough to generate infiltration into the cracks.

(3) Surficial movement is correlated to groundwater peaks above the threshold level.

These features gave rise to the following considerations:

(1) The rapid piezometric responses are attributed to an infiltration process through a superficial system of interconnected cracks. This system not only works as a fast flowpath from the ground surface to the water table, but is also capable of rapidly discharging the infiltrated water (Fig. 4). The depth of this crack system is assumed to correspond with the "threshold" level. The surficial movement seems to be related to this short-term hydrological regime, at least at this location.

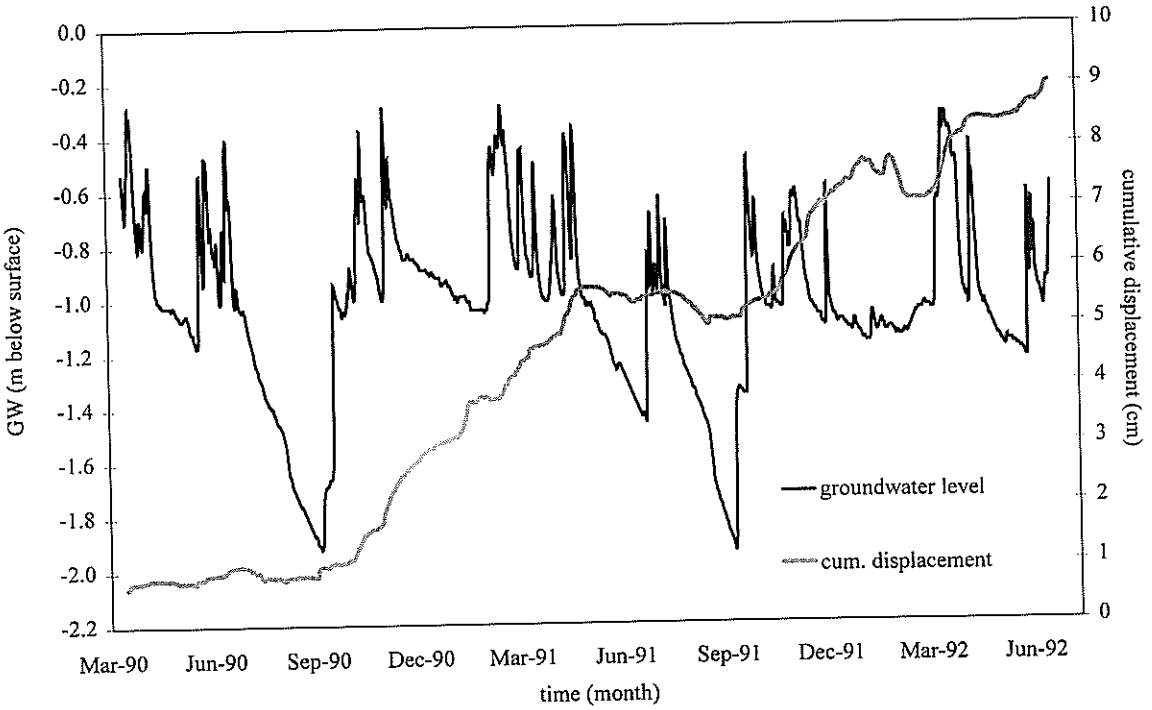

Fig. 3. Characteristic response of piezometers and extensometers on the Alverà landslide: example S5.

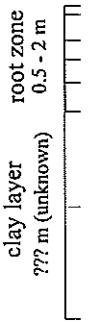

Fig. 4. Hydrol

(2) The extension of
to greater depth,
perforated sectio
vides short path
(Fig. 4), and is
the rapid ground
piezometers.

(3) The marked seas
of the fall of gro
be caused by a
matrix flow. Thi
from both (super
systems, reaches
of winter, and its
summer. The dr
end" cracks cou
head difference
these cracks an
level; in other
unsaturated part

(4) The failure of ma
tion events to p
suggests a water
root zone caused
must be replenisl
cracks can occur

Numerous soil pro
superficial, oxidized
layer. The depth of
with the depth of the
provides a possible p

vents. In the case of
a groundwater rise
s rapid as in other
ow the initial level is.
em not to be large
ation into the cracks.
rrelated to ground-
reshold level.

to the following

ponses are attributed
through a superficial
cracks. This system
t flowpath from the
ater table, but is also
arging the infiltrated
of this crack system
with the "threshold"
vement seems to be
hydrological regime,

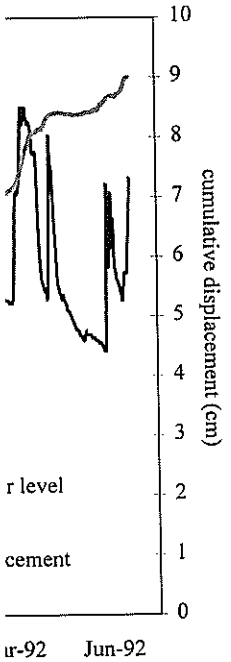

: example S5.

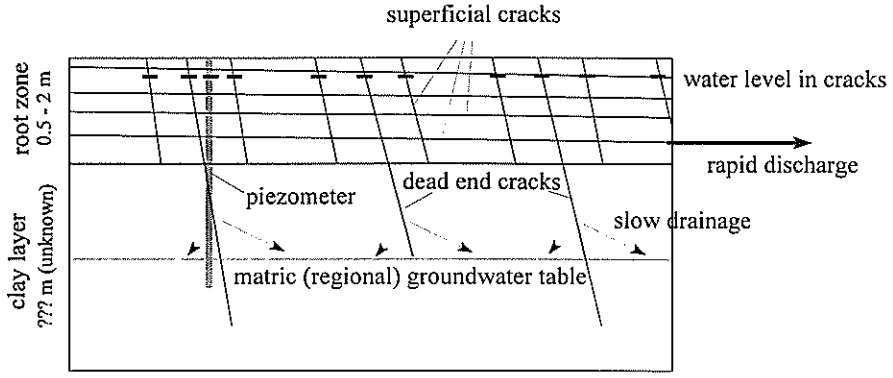

Fig. 4. Hydrological concept of the Alverà landslide, as inferred from groundwater and displacement data.

(2) The extension of occasional "dead-end" cracks to greater depth, where they may dissect the perforated sections of the piezometers, provides short pathways for infiltrating water (Fig. 4), and is a reasonable explanation for the rapid groundwater rises recorded by the piezometers.
(3) The marked seasonal difference in the rapidity of the fall of groundwater levels is believed to be caused by an annual cycle of regional matrix flow. This flow, which is independent from both (superficial and "dead end") crack systems, reaches its maximum level at the end of winter, and its minimum level at the end of summer. The drainage rate from the "dead end" cracks could then be explained by the head difference between the water level in these cracks and the regional groundwater level; in other words, the thickness of the unsaturated part of the clay layer (Fig. 4).
(4) The failure of many smaller summer precipitation events to produce any groundwater rise suggests a water deficit in the matrix of the root zone caused by evapotranspiration, which must be replenished before infiltration into the cracks can occur.

Numerous soil profiles showed a transition of a superficial, oxidized root zone into a reduced clay layer. The depth of this transition corresponds with the depth of the superficial crack system, and provides a possible physical representation of this system by plant roots and macropores. However, the deeper "dead end" cracks are more probably caused by movement of the landslide. These considerations are schematized into the following hydrological concept: a layer with a continuous, isotropic, permeable crack system overlies a layer with dead-end cracks in an otherwise clayey matrix. For convenience, these two layers will be referred to as the "root zone" and "clay layer", respectively.

4. Hydrological model

The hydrological concept outlined above was incorporated into a numerical model by adapting the model EPL (estimation of piezometric levels) (Hendriks, 1992). An application of this model to another landslide study is given by van Asch et al. (1996). The model consists of two linear reservoirs placed in series [Fig. 5(a)]. It was adapted such that the water level in the upper reservoir is influenced by the lower one whenever the latter is full [Fig. 5(b)]. In fact, the model now consists of one reservoir with two outlets, but for convenience the terms "upper/lower reservoir" will be used in the explanations. The following equations govern the level in the reservoirs:

$$dS=(P-Q_1-Q_2)\,dt, \tag{1}$$

$$Q_1=\frac{S-S_C}{k_1}, \tag{2a}$$

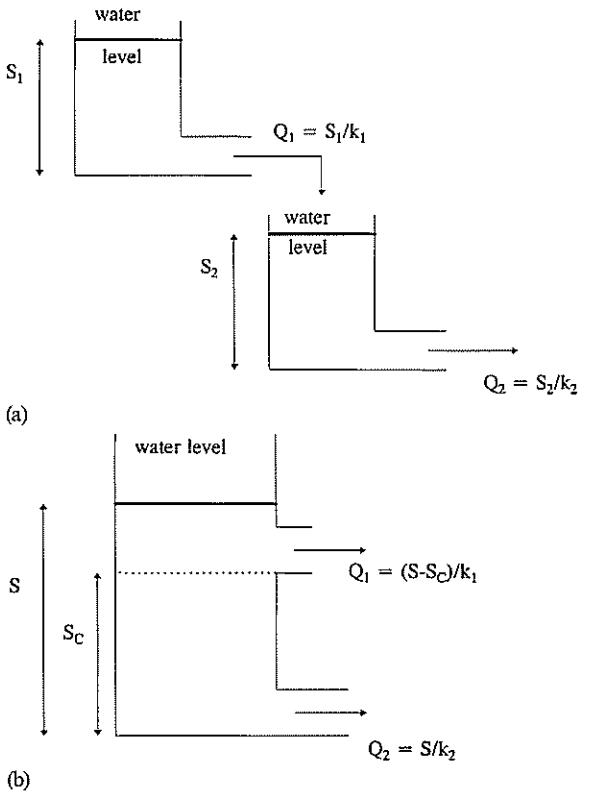

Fig. 5. (a) The EPL-model (Hendriks, 1992); (b) adaptation of the EPL-model for simulation of groundwater levels on the Alverà landslide.

$$Q_2 = \frac{S}{k_2}, \tag{2b}$$

where S is storage (L); P is the effective precipitation (L); Q_1 is the discharge from the upper reservoir ($L\,T^{-1}$); Q_2 is the discharge from the lower reservoir ($L\,T^{-1}$); S_C is maximum storage of the lower reservoir (constant) (L); and k_1, k_2 represent the discharge coefficients for upper and lower reservoirs, respectively (T).

If the upper reservoir is empty ($S \le S_C$), then $Q_1 = 0$, and Eqs. (1) and (2b) are combined to:

$$k_2\,\mathrm{d}Q_2 = (P - Q_2)\,\mathrm{d}t. \tag{3}$$

By discretizing $\mathrm{d}t$ to Δt, $\mathrm{d}Q_2$ to $Q_2(t+\Delta t) - Q_2(t)$ and Q_2 to $0.5\{Q_2(t+\Delta t) + Q_2(t)\}$, Eq. (3) becomes (Hendriks, 1992):

$$Q_2(t+\Delta t) = \frac{k_2 - 0.5\Delta t}{k_2 + 0.5\Delta t}\,Q_2(t) + \frac{1}{k_2 + 0.5\Delta t}\,P\Delta t. \tag{4}$$

The mean storage in a timestep is then given by:

$$0.5\{S(t+\Delta t) + S(t)\} = 0.5k_2\{Q(t+\Delta t) + Q(t)\}. \tag{5}$$

If the upper reservoir is not empty ($S \ge S_C$), then Eqs. (1), (2a) and (2b) are combined as:

$$k_2\,\mathrm{d}Q_2 = \left(P - \frac{k_2 Q_2 - S_C}{k_1} - Q_2\right)\mathrm{d}t. \tag{6}$$

By applying the same discretization, this can be rewritten as:

$$Q_2(t+\Delta t) = \frac{2k_1k_2Q_2(t) + \Delta t(2k_1P - k_1Q_2(t) - k_2Q_2(t) + 2S_C)}{2k_1k_2 + \Delta t(k_1 + k_2)} \tag{7}$$

and the mean storage can again be found with Eq. (5). A particular situation occurs when $S(t) < S_C$ and $S(t+\Delta t) > S_C$. In this case, Eq. (3) applies until S_C is reached; from then, Eq. (6) applies.

To calculate the fraction of the timestep T needed to reach S_C in this case, Eqs. (1) and (3) are combined to the differential equation (Q_1 still being zero):

$$\mathrm{d}S = \left(P - \frac{1}{k_2}S\right)\mathrm{d}t, \tag{8}$$

which can be solved to yield

$$t = -k_2 \ln\left(P - \frac{1}{k_2}S\right) + C. \tag{9}$$

The beginning of the timestep is defined as $t=0$, with S, the storage at the beginning of the timestep, known [$S(t=0)$]. The constant C is then known and Eq. (9) becomes:

$$t = k_2 \ln\left(P - \frac{1}{k_2}S(t=0)\right) - \ln\left(P - \frac{1}{k_2}S\right). \tag{10}$$

T is obtained by
remaining part o
equation is Eq. (7
of Δt. The mean
can then be calcula
The opposite si
$S(t+\Delta t) < S_C$] can
combining Eqs. (1
differential equatio
to groundwater lev
ity or storage capa

5. Application of th Alverà landslide

In the Alverà la
reservoir represent
reservoir the clay la
the landslide area
flow that was inferr
probably has a mu
the extent of this
properties are knov
to assess. Based
regional flow is ass
it must not be par
the reservoir model
cale. Therefore, it
boundary conditio
timestep, but varie
to a sinus-function
reservoir is physica
the dead-end crack
above the regional
from the cracks is
below the regional
surrounding the cr
to the annual cycl
table, the lower re
through the year. T
water table, the sm
reservoir S_C [Eq. (
charge from it since
[Eq. (2b)]. Dischar
remains unaffected
remains constant.
function describing

$$)+\frac{1}{k_2+0.5\Delta t}P\Delta t. \quad (4)$$

step is then given by:

$$\{Q(t+\Delta t)+Q(t)\}. \quad (5)$$

t empty ($S \geq S_C$), then combined as:

$$Q_2\Big)\,dt. \quad (6)$$

retization, this can be

$$_2(t)-k_2Q_2(t)+2S_C)}{+k_2)} \quad (7)$$

again be found with tuation occurs when $_C$. In this case, Eq. (3) d; from then, Eq. (6)

on of the timestep T case, Eqs. (1) and (3) ential equation (Q_1 still

$$(8)$$

ld

$$(9)$$

step is defined as $t=0$, ginning of the timestep, stant C is then known

$$-\ln\left(P-\frac{1}{k_2}S\right). \quad (10)$$

T is obtained by taking S_C for S. During the remaining part of the timestep, the governing equation is Eq. (7), but with $\Delta t^* = \Delta t - T$ instead of Δt. The mean storage for the whole timestep can then be calculated from $S(t)$, $S(t+\Delta t)$ and T. The opposite situation [i.e. $S(t) > S_C$ and $S(t+\Delta t) < S_C$] can be handled in a similar way by combining Eqs. (1) and (6) and solving the differential equation. Storage levels are converted to groundwater levels through division by a porosity or storage capacity parameter R.

5. Application of the hydrological model to the Alverà landslide

In the Alverà landslide case study, the upper reservoir represents the root zone and the lower reservoir the clay layer. The model comprises only the landslide area itself. However, the regional flow that was inferred from the piezometric records probably has a much larger feeding area. Neither the extent of this area, nor its geohydrological properties are known and both entities are difficult to assess. Based on the piezometric data, the regional flow is assumed to have an annual cycle; it must not be part of the drainage equations of the reservoir model, which work on a daily timescale. Therefore, it is incorporated as a bottom boundary condition which is constant during one timestep, but varies through the year, according to a sinus-function with a 1 year period. The lower reservoir is physically represented by that part of the dead-end crack system in the clay layer that is above the regional groundwater table. Drainage from the cracks is only possible from this part; below the regional groundwater table, the matrix surrounding the cracks is already saturated. Due to the annual cycle of the regional groundwater table, the lower reservoir expands and contracts through the year. The higher the regional groundwater table, the smaller the thickness of the lower reservoir S_C [Eq. (2a)] and the smaller the discharge from it since total storage S is also smaller [Eq. (2b)]. Discharge from the upper reservoir remains unaffected because $(S-S_C)$ in Eq. (2a) remains constant. The parameters of the sinus-function describing the regional water table are defined as follows: the yearly maximum is set mid-February and the yearly minimum half a period later, i.e. mid-August. These are the periods when the highest and lowest levels in the crack system of the clay layer are recorded. The maximum regional groundwater level is equal to the top of the clay layer (1 m below the ground surface), the minimum level was set at 2 m below the surface, which is slightly lower than the lowest recorded level (in August 1990). With this function, the regional groundwater level can be calculated as function of the time of year:

$$GW_{reg} = -1.50 - 0.5 \sin\left[\frac{2\pi}{365}\,daynumber\right], \quad (11)$$

where *daynumber* is $91+k365$ ($k=1,2,\ldots$) so that on 17 August $\sin[..]=1$.

Porosity values for the superficial and dead-end crack systems (R_1 and R_2) were estimated from ratios between effective precipitation and groundwater rise in borehole S5, for 16 events between 1989 and 1995. Only winter events were considered to minimize the difference between gross and effective precipitation. For example, in December 1995, 8.6 mm of rain caused a groundwater rise from -1.71 m to -1.43 m ($=280$ mm) in the clay layer, so R_2 equals $8.6/280=0.03$. In other words, 1 mm of effective precipitation would cause an increase in storage S of 1 mm, but an increase in groundwater level of about 33 mm. Assuming that leakage does not take place, such an unusually low R-value may be explained by the generation of local over-land flow above the soil matrix which then reaches a crack and infiltrates after all. Thus, the crack system receives more infiltration than its areal equivalent.

Groundwater flow perpendicular to the slope is neglected. Support for this assumption comes from the observation that the major streams bordering the landslide are deep enough to capture most of the flow through the superficial crack system. A possible lateral component in regional matrix flow is incorporated in the sinus function mentioned above.

The conversion of gross to effective precipitation is problematic because of the lack of data. Yet evapotranspiration is probably important because

many smaller summer precipitation events are apparently buffered by a water deficit in the root zone. In the model, a fraction of precipitation is subtracted, followed by a fixed value, where the former represents interception (only occurring during precipitation) and the latter transpiration by vegetation (which occurs also on dry days). The interception percentage is set at 15% during the season of maximum development of the grass cover (June–September). In the other seasons, interception is neglected. Transpiration is set at 2 mm day^{-1} provided the mean daily air temperature exceeds 5°C, otherwise it is neglected. A negative precipitation surplus is entirely subtracted from the water storage in the matrix of the root zone provided this water storage is maximal; if not, then the subtracted amount linearly decreases with decreasing storage (Thornthwaite and Mather, 1957). Thus, a water deficit is built up, which must be replenished before infiltration can occur into the cracks. The maximum water storage in the root zone was derived from pF curves measured on 25 root zone samples.

Finally, snow must be considered as well because it is the main mode of precipitation during winter. The meteorological station on the landslide records snow water equivalent (SWE). Snowmelt is governed by the following equation:

$$M = \min[\mathrm{SWE}, c(T - T_0)], \quad (12)$$

where M is the snowmelt rate (mm d^{-1}); T is the mean daily air temperature (°C); T_0 is the temperature below which no snowmelt occurs (°C); and c is the snowmelt coefficient (mm day^{-1}°C^{-1}). This "degree-day method" is used, for example, by Bergström (1976). Padt (1987) obtained calibration values of T_0 and c for the Dolomites; these are shown in Table 2.

To help the reader, a one-timestep example of the modelling procedure is included in Appendix A, using input parameter values from Table 2, which shows the model parameter input values that produced the best calibration fit. For calibration, the S5 piezometer series was chosen because it has the longest temporal span (7 years). The model was calibrated for the period August 1992–September 1993, and validated for May 1990–July 1992.

6. Results and discussion of the hydrological model

Fig. 6 shows the simulation results. The response pattern is reproduced very well, although some recorded peaks are underestimated or missed. In terms of model robustness, the parameters k_1 and k_2 are the two calibration parameters. However, model output is quite sensitive to changes in the porosity values. A satisfactory physical explanation of the low porosity values is still lacking. Even if the supposition of over-land flow infiltration into cracks stated in Section 5 holds true, considerable simplification is introduced by using constant instead of transient values; swell–shrink behaviour of clay and organic material may temporarily change the porosity of the crack system. These are important reasons for detailed field research on this subject.

Another important research topic is the measurement of evapotranspiration parameters. Despite the good results produced, values for these parameters were a rough guess; if the values used are unrealistic, they could offset another source of error, thus producing reasonable results after all. This exercise shows the difficulty of modelling landslide hydrology: even if one of the simplest possible conceptual hydrological models is applied on a very well-instrumented landslides, several processes remain unclear or unverified.

7. Slope stability modelling

In the classical approach to slope stability analysis, soil strength is regarded as a unique resisting force. As a direct result, movement starts as soon as the equilibrium between driving and resisting forces is modified by a finite pore-water pressure increase acting along the slip surface. At this moment, a net force difference between driving and resisting forces becomes available. This net force is constant and the landslide moves subject to constant acceleration with an infinitely increasing velocity.

This is in contrast with field evidence, which shows that the velocity becomes constant with time provided that the pore pressures along the slip surface remain constant. In order to give a

Table 2
Input parameters to th

Parameter
Precipitation, temperat
Snowmelt threshold ter
Coefficient of snowmelt
Potential evapotranspir
Interception
Thickness upper reserv
Thickness lower reserv
Discharge coefficient u
Discharge coeffcicient l
Porosity upper reservoi
Porosity lower reservoi

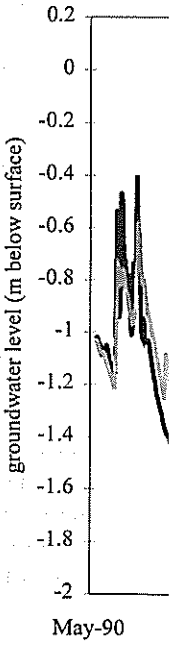

clear explanation
viscous resisting fo
illonitic clay comp
considered. The d
visco-plastic rheol
1996b) led to the
tional resistance is
moving with a ve

Table 2
Input parameters to the hydrological model

Parameter	Symbol	Value
Precipitation, temperature	P, T	Transient
Snowmelt threshold temperature	T_0	−0.3 (°C)
Coefficient of snowmelt	c	1.9 (mm d^{-1}°C)
Potential evapotranspiration	ET	2 (mm d^{-1}) (if T>5°C)
Interception	I	0.15 P (summer only)
Thickness upper reservoir	D_1	1.00 m
Thickness lower reservoir	D_2	Minimum 0 m; maximum 2 m (sin function)
Discharge coefficient upper reservoir	k_1	10 (d)
Discharge coeffcicient lower reservoir	k_2	50 (d)
Porosity upper reservoir	R_1	0.06 (–)
Porosity lower reservoir	R_2	0.03 (–)

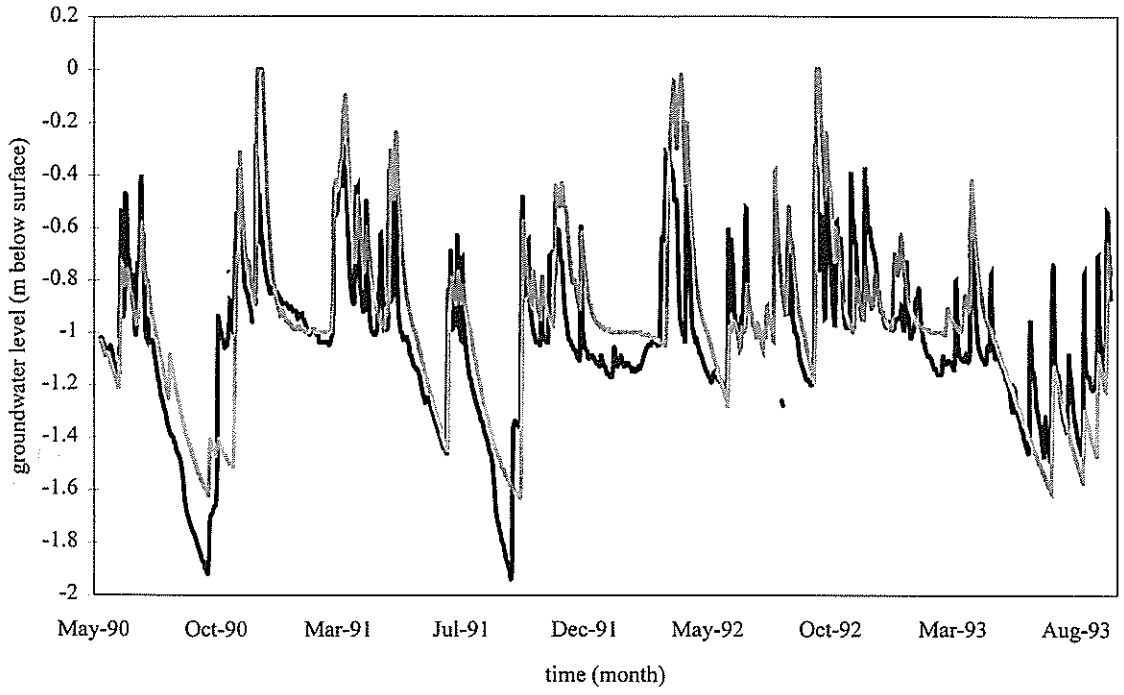

Fig. 6. Predicted (grey) and observed (black) groundwater levels.

clear explanation of this behaviour, the effects of viscous resisting forces developing in the montmorillonitic clay composing the landslide had to be considered. The development of a Bingham-type visco-plastic rheological model (Angeli et al., 1996b) led to the conclusion that once the frictional resistance is overcome, the landslide starts moving with a velocity controlled by a viscous resistance term. The difference between driving and resisting forces in terms of stresses now becomes (see also Fig. 7):

$$-\left(\tau_f+\frac{\eta}{z}\frac{\mathrm{d}s}{\mathrm{d}t}\right)=\frac{ma}{A}=\frac{m}{A}\frac{\mathrm{d}v}{\mathrm{d}t}, \qquad (13)$$

where τ is the driving stress (M LT^{-2}); τ_f is the

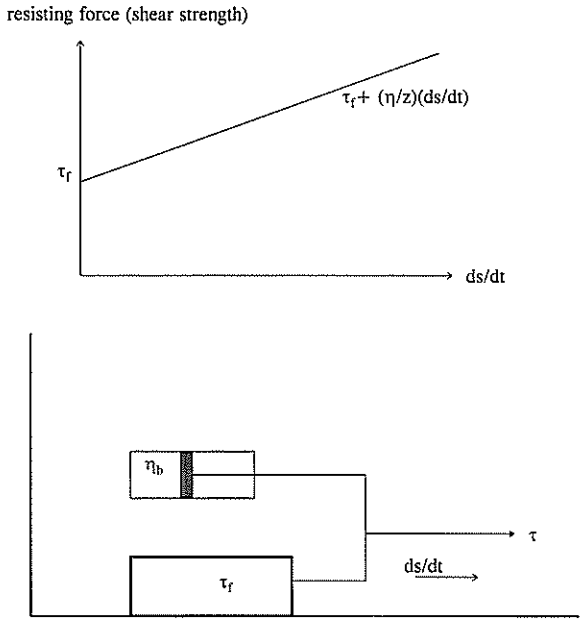

Fig. 7. Principle of the visco-plastic rheological model (Angeli et al., 1996b).

frictional resistance (M LT^{-2}); η is the coefficient of viscosity (M LT^{-1}); z is the thickness of deforming soil around the slip surface (L); v is the velocity (L T^{-1}); m is the sliding mass (M); a is the acceleration constant (L T^{-2}); A is the area of the slip-plane portion corresponding to a sliding mass m; (L^2); and t is time (T).

Integration of Eq. (13) yields:

$$v = \frac{X - e^{\ln a - Yt}}{Y}, \qquad (14)$$

where

$$X = \frac{A}{m(\tau - (\sigma_{tot} - u)\tan\phi')} \text{ and } Y = \frac{A}{m}\frac{\eta}{z},$$

and $(\sigma_{tot} - u)\tan\phi'$ is the residual shear strength (M LT^{-2}); u_{tot} is the total normal stress (M LT^{-2}); and u is pore pressure (M LT^{-2}).

Because the landslide has failed already, the frictional resistance τ_f equals the residual shear strength. The velocity becomes dependent on the pore pressure variation only, when all other parameters are constant. Because the thickness of the moving part of the landslide (5 m) is small compared with its length (1500 m), the infinite slope model can be adopted to calculate τ and σ from bulk unit weight, slope angle and residual angle of internal friction along the slip surface (ϕ') of the landslide (Table 1). Pore pressure u can be calculated from recorded groundwater levels, slope angle and unit weight of water. Due to the difficulty of seperately determining η and z with laboratory or in situ tests, they are combined as the term η/z on which the model was calibrated. The term is analogous to Bingham's expression for viscous resistance η_B. For more details about the model and its calibration see Angeli et al. (1996b).

In addition, field observations revealed different pore pressure threshold values for triggering the landslide movement. On the basis of laboratory tests carried out on the montmorillonitic clay, these thresholds were attributed to soil strength regain (thixotropy). Furthermore, it was found that the longer the rest time of the landslide, the higher the strength regain relative to the residual strength. This implies that landslide movement after a long period of rest is triggered only when the pore pressure exceeds the value at which the landslide stopped. Direct shear tests revealed that the net difference between the two pore pressure thresholds, after identical periods of rest, exactly corresponded to the soil strength regain that was observed in the field. In this way, a more refined model capable of explaining all the phenomena operating in the field was obtained. Using the observed pore-pressure series and strength regain data, it was possible to reproduce the observed trend of landslide displacement, again of S5 (Angeli et al., 1996b).

8. Linked hydrological and slope stability modelling

The simulated groundwater levels were used as input to the stability model in order to directly obtain displacement values as a function of precipitation. Results are shown in Fig. 8 for the period September 1990–September 1993, again for borehole S5. The correspondence between modelled and observed deformation is good except in the second half of 1992. This is probably due to a decreased reliability of the displacement measure-

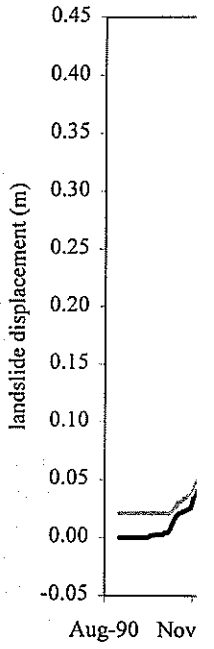

ments in this perio
results are satisfacto
opments and refinem

9. Conclusions

The use of the con
stability model so f
conclusions.

(1) It must be real
carried out on or
record only. The
model depends c
against the other
of strongly modi
Although the otl
terns, they are n
out a reliable cal

(2) The good perfor
supports the ph
processes assume
some of them ne

m), the infinite slope
alculate τ and σ from
e and residual angle of
lip surface (ϕ') of the
essure u can be calcu-
ndwater levels, slope
er. Due to the difficulty
and z with laboratory
nbined as the term η/z
alibrated. The term is
xpression for viscous
tails about the model
li et al. (1996b).
tions revealed different
lues for triggering the
ie basis of laboratory
montmorillonitic clay,
buted to soil strength
ermore, it was found
e of the landslide, the
elative to the residual
t landslide movement
is triggered only when
he value at which the
iear tests revealed that
the two pore pressure
eriods of rest, exactly
engths regain that was
is way, a more refined
ig all the phenomena
obtained. Using the
es and strength regain
produce the observed
cement, again of S5

lope stability modelling

ter levels were used as
el in order to directly
as a function of precipi-
n Fig. 8 for the period
1993, again for bore-
nce between modelled
is good except in the
is probably due to a
displacement measure-

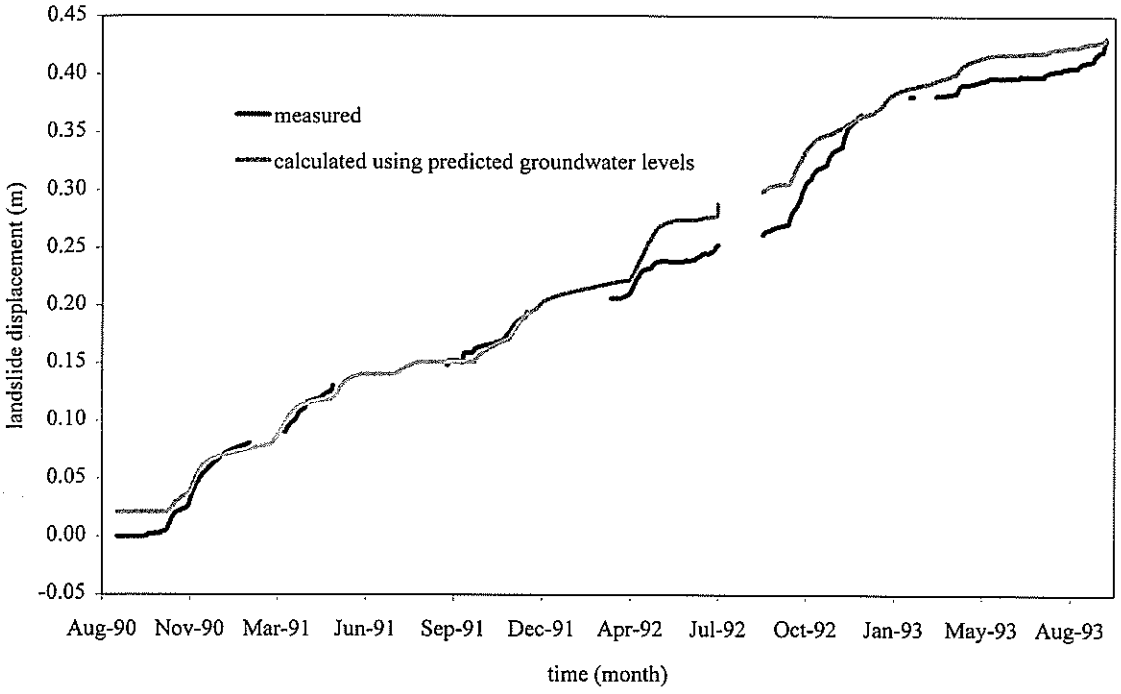

Fig. 8. Predicted and observed landslide displacement.

ments in this period. Otherwise, the modelling results are satisfactory, and encourage new developments and refinements.

9. Conclusions

The use of the combined hydrological and slope stability model so far has led to the following conclusions.

(1) It must be realized that a validation was carried out on one groundwater–displacement record only. The performance of the combined model depends on the success of a validation against the other records without the necessity of strongly modifying the model parameters. Although the other records have similar patterns, they are not yet long enough to carry out a reliable calibration.

(2) The good performance of the combined model supports the physical interpretation of the processes assumed in the two models, although some of them need to be better quantified and verified in the field. These processes may be representative for similar low-gradient clayey slopes, which are widespread in the Italian Dolomites and many other mountain regions. Therefore, the model has perspectives for future use in regional landslide studies, provided the condition from conclusion 1 is fulfilled.

(3) The model can be applied for civil protection purposes or climate impact studies in the future. In fact, the prediction of landslide movement on the basis of precipitation and the possibility to provide a kind of an alarm in case of extreme precipitation events can represent in some practical cases a powerful tool in order to preserve safety in densely populated areas affected by large landslides.

Acknowledgment

This paper is part of the CEC Environment Research Programme on Temporal Stability and

Activity of Landslides in Europe with respect to Climatic Change (TESLEC), contract number EV5V-CT94-0454. We are grateful to Drs Andy Collison and Maia Ibsen (King's College London), Dr Tullia Bonomi (University of Milan) for their contribution in collecting the field data, and to Dr Theo van Asch (University of Utrecht) for his useful suggestions. Special thanks are due to Dr Thom Bogaard (University of Utrecht) who came up with some invaluable suggestions.

Appendix A

One-timestep example of hydrological modelling procedure. Model parameters, as mentioned in the equations in the text, should be assigned values taken from Table 2

On 20 May 1990, mean air temperature was 7.9°C, and total precipitation was 9.8 mm. First, effective precipitation is calculated from processes. If snow were available, snowmelt would be [Eq. (12)]: $1.9(7.9--0.3)=15.6\ \text{mm d}^{-1}$, and total precipitation for this day would increase to 25.4 mm. However, no snow was present on the previous day, so the stored snow water equivalent, and hence snowmelt, is zero.

Next, evapotranspiration losses are calculated. In this time of the year, the grass vegetation is still short; thus, interception is neglected. Because mean temperature exceeds 5°C, potential evapotranspiration is $2\ \text{mm d}^{-1}$. Actual evapotranspiration is smaller than potential evapotranspiration if the water storage in the root zone is maximal; this difference becomes larger when the soil becomes drier. At the beginning of the day, however, the matrix was saturated; therefore, potential equals actual evapotranspiration. Effective precipitation becomes (1−interception)P−actual evaporation $=1.00\times9.8-2=7.8$ mm. This amount infiltrates the landslide. Because the root zone is saturated, as stated above, all this water enters the crack system. If daynumber 2 is the 20th May; the regional groundwater table becomes [Eq. (11)]:

$$GW_{reg}=-1.50-0.5\sin(2\pi/365)2=-1.52\ \text{m}.$$

Suppose that the groundwater level at the beginning of the day (timestep) is within the clay layer: $G(t)=-1.40$ m. Because the apparent porosity of the dead-end crack system in the clay layer is 0.03 (Table 2), storage above the regional water table is: $S(t)=(-1.40--1.52)\times0.03=0.0036$ m. Eq. (2b) applies with, according to Table 2, $k_2=50$ days and $Q_2(t)$ becomes $0.0036/50=7.2\times10^{-5}\ \text{m d}^{-1}$. With Eq. (4), $Q(t+\Delta t)$ at the end of the timestep can be calculated, with $\Delta t=1$ day, $Q_2(t)=7.2\times10^{-5}\ \text{m d}^{-1}$, $P=7.8$ mm $=0.0078$ m and $k_2=50$ days: $Q(t+\Delta t)=2.3\times10^{-4}\ \text{m d}^{-1}$. Applying Eq. (2b) backwards yields $S(t+\Delta t)=2.3\times10^{-4}\times50=0.011$ m. The groundwater level at the end of the timestep is now calculated through division by the porosity: $G(t+\Delta t)=0.011/0.03-1.52=-1.15$ m. Because this value is still below the boundary between the root zone and clay layer (at −1.00 m), the use of only Eq. (4) was justified. Had $G(t+\Delta t)$ become higher than −1.00 m, then the procedure should have to be repeated, using Eqs. (7) and (10). Finally, mean groundwater level for the day is calculated: $(-1.40-1.15)/2=-1.28$ m.

References

van Asch, T.W.J., Hendriks, M.R., Hessel, R., Rappange, F.E., 1996. Hydrological triggering conditions of landslides in varved clays in the French Alps. Eng. Geol. 42, 239–251.

Angeli, M.G., Menotti, R.M., Pasuto, Silvano, S., 1992. Landslide studies in the Eastern Dolomites Mountains, Italy. In: Bell, D.H. (Ed.), Landslides. Proceedings of the 6th International Symposium on Landslides, Christchurch, New Zealand, Vol. 1. Balkema, Rotterdam, pp. 275–282.

Angeli, M.G., Gasparetto, P., Menotti, R.M., Pasuto, A., Silvano, S, 1996a. Examples of mudslides on low-gradient clayey slopes. In: Senneset, K. (Ed.), Landslides. Proceedings of the 7th International Symposium on Landslides, Trondheim (Norway), Vol. 1. Balkema, Rotterdam, pp. 141–145.

Angeli, M.G., Gasparetto, P., Menotti, R.M., Pasuto, A., Silvano, S., 1996b. A visco-plastic model for slope analysis applied to a mudslide in Cortina d'Ampezzo, Italy. Q. J. Eng. Geol. 29, 233-240.

Angeli, M.G., Pasuto, A., Silvano, S., 1996c. Landslide hazard in high mountain areas: case histories in the Italian Dolomites. J. Geol. Soc. China 39 (4), 401-422.

Bergström, S., 1976. Development and Application of a Conceptual Runoff Model for Scandinavian Catchments. SMHI Report RHO 7, Norrköping.

Deganutti, A.M., Gasparetto, P. 1992. Some aspects of a mudslide in Cortina, Italy. In: Bell, D.H. (Ed.), Proceedings of the 6th International Symposium on Landslides

Christchurch (New Z
pp. 373–378.
Gasparetto, P., Panizza,
M., 1994. Research
Casale, R., Fantechi,
Occurrence and Fore
Community (Final R
European Commisior
Gasparetto, P., Mosseln
mobility of the Alver
Geomorphology 15,
Hendriks, M.R., 1992.
EPL model. Internal
ment of Physical Geo
Hennrich, K., 1995. Ana

Christchurch (New Zealand), Vol. 1. Balkema, Rotterdam, pp. 373–378.
Gasparetto, P., Panizza, M., Pasuto, A., Silvano, S., Soldati, M., 1994. Research in the Cortina d'Ampezzo area. In: Casale, R., Fantechi, R., Flageollet, J.C. (Eds.), Temporal Occurrence and Forecasting of Landslides in the European Community (Final Report). Science Research Development, European Commision, Brussels, pp. 741–768.
Gasparetto, P., Mosselman, M., van Asch, T.W.J., 1995. The mobility of the Alverà landslide (Cortina d'Ampezzo, Italy). Geomorphology 15, 327–335.
Hendriks, M.R., 1992. Estimation of piezometric levels: the EPL model. Internal manual, Utrecht University, Department of Physical Geography.
Hennrich, K., 1995. Analysis of the relation between precipitation and groundwater of the Alverà landslide, Cortina d'Ampezzo, Italy. M.Sc. Thesis, University of Heidelberg (in German).
Padt, F.J.G., 1987. Hydrological regionalisation applied to snowmelt and snowmelt runoff. Internal report, Earth Sciences, Free University, Amsterdam.
Panizza, M., Pasuto, A., Silvano, S., Soldati, M., 1996. Time occurrence and activity of landslides in the area of Cortina d'Ampezzo (Dolomites, Italy). In: Soldati, M. (Ed.), Landslides in the European Union. Geomorphology 15, 311–326.
Thornthwaite, C.W., Mather, J.R., 1957. Instructions and tables for computing potential evapotranspiration and the water balance. Drexel Institute of Technology, Laboratory of Climatology. Publications in Climatology, Vol. 10 (3), Centerton, NJ, pp. 185–309.

he apparent porosity
:m in the clay layer is
ve the regional water
.52) × 0.03 = 0.0036 m.
ccording to Table 2,
becomes 0.0036/50 =
:q. (4), $Q(t+\Delta t)$ at
m be calculated, with
10^{-5} m d^{-1}, $P = 7.8$
: 50 days: $Q(t+\Delta t) =$
; Eq. (2b) backwards
$^{4} \times 50 = 0.011$ m. The
:nd of the timestep is
/ision by the porosity:
! = −1.15 m. Because
boundary between the
t −1.00 m), the use of
Had $G(t+\Delta t)$ become
the procedure should
ıg Eqs. (7) and (10).
r level for the day is
! = −1.28 m.

, Hessel, R., Rappange, F.E.,
conditions of landslides in
s. Eng. Geol. 42, 239–251.
ıuto, Silvano, S., 1992. Land-
lomites Mountains, Italy. In:
:oceedings of the 6th Interna-
ıslides, Christchurch, New
terdam, pp. 275–282.
Menotti, R.M., Pasuto, A.,
ıf mudslides on low-gradient
Ed.), Landslides. Proceedings
ɔsium on Landslides, Trond-
na, Rotterdam, pp. 141–145.
Menotti, R.M., Pasuto, A.,
ıstic model for slope analysis
a d'Ampezzo, Italy. Q. J. Eng.

), S., 1996c. Landslide hazard
histories in the Italian Dolo-
(4), 401-422.
ıt and Application of a Con-
ıdinavian Catchments. SMHI

1992. Some aspects of a mud-
l, D.H. (Ed.), Proceedings of
ımposium on Landslides.

NOTE TO CONTRIBUTORS

A detailed Guide for Authors is available upon request. Please pay attention to the following notes:

Language

The official language of the journal is English, but occasional articles in French and German will be considered for publication. Such articles should start with an abstract in English, headed by an English translation of the title. An abstract in the language of the paper should follow the English abstract. English translations of the figure and table captions should also be given.

Preparation of the text

(a) The manuscript should preferably be prepared on a word processor and printed with double spacing and wide margins and include an abstract of not more than 500 words.
(b) Authors should use IUGS terminology. The use of S.I. units is also recommended.
(c) The title page should include, the name(s) of the author(s) their affiliations, fax and e-mail numbers. In case of more than one author, please indicate to whom the correspondence should be addressed.

References

(a) References in the text consist of the surname of the author(s), followed by the year of publication in parentheses. All references cited in the text should be given in the reference list and vice versa.
(b) The reference list should be in alphabetical order.

Tables

Tables should be compiled on separate sheets and should be numbered according to their sequence in the text. Tables can also be sent as glossy prints to avoid errors in typesetting.

Illustrations

(a) All illustrations should be numbered consecutively and referred to in the text.
(b) Drawings should be lettered throughout, the size of the lettering being appropriate to that of the drawings, but taking into account the possible need for reduction in size. The page format of the journal should be considered in designing the drawings.
(c) Photographs must be of good quality, printed on glossy paper.
(d) Figure captions should be supplied on a separate sheet.
(e) If contributors wish to have their original figures returned this should be requested in proof stage at the latest.
(f) Colour figures can be accepted providing the reproduction costs are met by the author. Please consult the publisher for further information.

Page Proofs

One set of page proofs will be sent to the corresponding author, to be checked for typesetting/editing. The author is not expected to make changes or corrections that constitute departures from the article in its accepted form. Proofs should be returned within 3 days. The office fax number is: +31-20-4852459.

Reprints

Fifty reprints of each article published are supplied free of charge. Additional reprints can be ordered on a reprint order form which will be sent to the corresponding author upon receipt of the accepted article by the publisher.

SUBMISSION OF MANUSCRIPTS

Three copies should be submitted to: Editorial Office *Engineering Geology*, P.O. Box 1930, 1000 BX Amsterdam, The Netherlands. *Illustrations:* Please note that upon submission of a manuscript three sets of all photographic material printed SHARPLY on GLOSSY PAPER or as HIGH-DEFINITION LASER PRINTS must be provided to enable meaningful review. Photocopies and other low-quality prints will not be accepted for review.
The indication of a fax and e-mail number on submission of the manuscript could assist in speeding communications. The fax number for the Amsterdam office is +31-20-4852696.

Authors in Japan please note: Upon request, Elsevier Science Japan will provide authors with a list of people who can check and improve the English of their paper (*before submission*). Please contact our Tokyo office: Elsevier Science Japan, 20-12 Yushima 3-chome, Bunkyo-ku, Tokyo 113; Tel. (03)-3833-3821; Fax (03)-3836-3064.

Submission of an article is understood to imply that the article is original and unpublished and is not being considered for publication elsewhere.

SUBMISSION OF ELECTRONIC TEXT

Authors are requested to submit the final text on a 3.5" or 5.25" diskette. Both double density (DD) and high density (HD) diskettes are acceptable. Make sure, however, that the diskettes are formatted according to their capacity (HD or DD) before copying the files onto them. As with the requirements for manuscript submission, the main text, list of references, tables and figure captions should be stored in separate text files with clearly identifiable file names. The format of these files depends on the word processor used. Texts written with Display Write, MultiMate, Microsoft Word, Samna Word, Sprint, T_EX, Volkswriter, Wang PC, WordMARC, WordPerfect and Wordstar or supplied in DCA/RFT, or DEC/DX format can be readily processed. In all other cases the preferred format is DOS text or ASCII. It is essential that the name and version of the word processing program, the type of computer on which the text was prepared, and the format of the text files are clearly indicated.

Authors are encouraged to ensure that the contents of the diskette correspond exactly to the contents of the hard copy manuscript. Discrepancies can lead to proofs of the wrong version being made. The word processed text should be in single column format. Keep the layout of the text as simple as possible; in particular, do not use the word processor's options to justify or to hyphenate the words.

If available, electronic files of the figures should also be included on a separate floppy disk.

Fractal Models in the Earth Sciences

by G. Korvin

"A fractal is a mathematical set or object whose form is extremely irregular and/or fragmented at all scales." So reads Mandelbrot's definition of the term which he coined and widely popularised in his famous monographs. This volume presents the first systematic summary of the fractal models that have been proposed to explain the irregular features and phenomena of the Earth — from meandering rivers and rugged coastlines to the pore space of reservoir sandstones and the prediction of earthquakes. No previous knowledge of fractals is assumed. Connections and analogies with other fields of natural and technical sciences (physics, biology, fractography, etc.) are always pointed out. More than 300 illustrations are included, demonstrating how fractal geometry reveals astonishing similarities between natural phenomena at widely different scales. The precise description of mathematical algorithms; the exhaustive list of references containing more than 1000 items and covering all geological/geophysical applications of fractals to the end of 1989; and the well-organized Author and Subject Indices with cross references make the work an indispensable reference book for anyone using fractals to describe irregular data sets.

The readership for this book is wide and includes: geological scientists, oceanographers, and meteorologists involved in describing and analysing irregular spatial data; as well as applied mathematicians, physicists and computer scientists looking for new fields of research.

Contents: Preface. 1. What on Earth fractal? The self-similarity of rivers. How long is the Vistula river? The paradox of tortuosity: permeability of kaolinite-bearing sandstones. The permeability of shaly sandstones. Basic concepts of percolation theory. Percolation models of rock permeability. Deadly quarrels and coastlines. The coastline of Britain. Fractal model of coastal erosion. Bifractal coastlines. The perimeter-area rule of Mandelbrot. Islands and lakes. The fractal shape of clouds. The "slit island" analysis of fracture surfaces. Mathematical appendix. The functional equations of similarity. Fractal curves are hot. References.
2. Fractals in Flatland: a romance of < 2 dimensions. The paradox of sedimentation rate. Stratigraphic hiatuses and sedimentation rate. From the Cantor dust to the Devil's staircase. A fractal model for stratigraphic hiatuses. Sadler's model of unsteady sedimentation and its fractal generalisation. Fractal analysis along a line: slip lines and fractures. Strange attractors, aggregates and geophysical networks. Fractal characterisation of geophysical measuring networks. Fractals in the plane: fractures - earthquakes - volcanoes. Cellular structures. Fracture networks, faults and earthquakes. Mathematical appendix. Different kinds of fractal dimensions and their numerical. References.
3. Korcak's law and fragmentation theory. The size-frequency relation for islands, lakes and caves. Fragmentation: from broken sea ice to the distribution of galaxies. The fractal theory of fragmentation. The Renormalization Group (RNG) model of rock fragmentation. Maximum-entropy people and fractal people. References.
4. Fractal surfaces. Fractal surfaces everywhere. Simple geometrical models of fractal surfaces. Analytical treatment of fractal surfaces. Wave scattering from fractal surfaces. Fractal models of porous rocks. Why are the pores fractal rather than smooth? Multifractal measures - not for the squeamish. References. 5. Of time and change. Paradoxes of time. The puzzle called the Hurst phenomenon. Paradoxes of the 1/f noise. On growth and form. References. Author index. Subject index.

1992 408 pages
US $ 127.75 / Dfl. 220.00
ISBN 0-444-88907-8

Elsevier Science Publishers
P.O. Box 1930
1000 BX Amsterdam
The Netherlands

P.O. Box 945
Madison Square Station
New York, NY 10160-0757

The Dutch Guilder (Dfl.) prices quoted apply worldwide. US $ prices quoted may be subject to exchange rate fluctuations. Customers in the European Community should add the appropriate VAT rate applicable in their country to the price.

ELSEVIER
SCIENCE PUBLISHERS